Transient Electromagnetic Response of Conductive Media Modeling and Inversion Based on Fictitious Wave Domain Method

Xiaoyu Zhao, Guofu Wang*, Faquan Zhang, Jincai Ye,

School of Information and Communication, Guilin University of Electronic Technology, Guilin 541004, China
e-mail: zhao_xiaoy@qq.com; guofwang@126.com; zhangfq@guet.edu.cn; kingsey@126.com.

Yiyu Zhan

School of Civil Engineering Institute, Putian University, Putian 351100, China
e-mail: 378281365@qq.com.

ABSTRACT

With the deep research on the existing and developing methodologies in seismology applied to the transient electromagnetic (TEM) method, the study of TEM fictitious wave domain method has become a hotspot in the field of electromagnetic (EM) exploration. We introduce a new and potentially useful method for computing TEM responses of subsurface conductivity distributions. Its key features are based on a correspondence principle relating diffusive wave field and fictitious wave field. Specifically, the data of diffusive EM region is transformed into its corresponding fictitious wave domain. The fictitious wave field transformation is implemented by using the method of preconditioned regularized conjugate gradient (PRCG). We also show that the correspondence principle can be extended to include not only EM fields but also the electromotive force (EMF). This scheme can deal well with the first class Fredholm integration equation and avoid segmentation of TEM time signals. The characteristics of fictitious wave field are analyzed. The performance of the p7roposed method is illustrated by some numerical experiments on synthetic wave field records and a theory model.

KEYWORDS: Transient electromagnetic (TEM), fictitious wave field, correspondence principle， preconditioned regularized conjugate gradient (PRCG) method

INTRODUCTION

At present, TEM method has demonstrated huge capacity in mineral exploration [1], [2], hydrocarbon exploration [3], groundwater sounding [4], [5], geological mapping [6], [7], accurate advanced detection of aquifer structure [8]-[10] and so on. The TEM response modeling and inversion play an important role in all of these geophysical techniques.

For TEM modeling and inversion, the methods can be divided into two kinds of integral and differential equation techniques. Raiche used integral equation approach for 3-D modeling [11]. Cox used an integral equation technique and cosine transform to compute the time-domain responses and

sensitivities [12]. In this method, the resulting matrix is full and generally asymmetric. In addition, each element of the matrix is derived from a combination of Green's functions whose computation is complications. Differential equation techniques were used by Lines for magnetotelluric (MT) solutions, and improved in power and efficiency by Reddy [13]. Goldman employed the finite-difference (FD) method with implicit time-stepping techniques for 2-D TEM modeling [14]. Sasaki applied the FD technique in frequency domain for forward solution and sensitivity [15].

A remarkable method based on a correspondence principle relating the diffusive and fictitious wave fields has mainly been developed for the controlled-source EM and MT modeling these days [16]. It shows the great potential to model TEM response. This is so-called the TEM fictitious wave domain method. In 1972, Kunetz in the study of MT interpretation and inversion found a similar relationship between the diffusion EM equation and wave equation [17]. Lavrent'ev first deduced the mathematical relationship [18]. Latter, Lee used the singular value decomposition (SVD) algorithm to implement the wave field transformation [19]. To deal with the first class Fredholm integration equation, Li made a segmentation on TEM time signals, and then the data transformation of fictitious wave field for each segmentation TEM signal was achieved by using regularization algorithm [20].

In this paper, we focus on TEM response of conductive media modeling and inversion. A preconditioned regularized conjugate gradient fictitious wave domain (PRCG-FWD) method is presented. The performance is tested numerically by using some synthetic wave field records and a theory model. We first show the correspondence principle relating the diffusive EM fields in the time domain and its corresponding fictitious wave fields in the fictitious time domain. The correspondence principle presented here has been generalized to include EMF. Transforming data from diffusive TEM region to its corresponding fictitious wave domain is implemented by PRCG method.

THEORY

TEM modeling based on correspondence principle

For typical earth conductivities, the conduction current is orders of magnitude greater than the displacement current. The displacement current is negligible [19], and the quasi-static Maxwell's equations are as follows:

$$\nabla \times H = \sigma E + J \,, \tag{1}$$

$$\nabla \times E = -\mu \partial_t H - K \,, \tag{2}$$

where μ is assumed to be constant and equal to the value in free space. ∂_t is derivative operator in the time t direction. The external sources are electric current density J and magnetic current density K.

According to equations (1) and (2), the following equations can be derived

$$\nabla \times \nabla \times H + \mu\sigma \partial_t H = S_H \,, \tag{3}$$

$$\nabla \times \nabla \times E + \mu\sigma \partial_t E = S_E \,, \tag{4}$$

where the source terms S_H and S_E, identified as

$$S_H = \nabla \times J - \sigma K \,, \tag{5}$$

$$S_E = -\mu \partial_t J - \nabla \times K \,, \tag{6}$$

are assumed to be causal. Throughout the derivation the medium is considered linear and isotropic. We now introduce the EM fields of the fictitious wave domain: E^U and H^U, which we call fictitious wave fields, such that

$$\nabla\times\nabla\times H^U+\mu\sigma\partial_{t'}^2H^U=S_{H^U}, \tag{7}$$

$$\nabla\times\nabla\times E^U+\mu\sigma\partial_{t'}^2E^U=S_{E^U}, \tag{8}$$

where $S_E{}^U$ and $S_H{}^U$ are the source terms of the fictitious wave fields E^U and H^U, respectively. $\partial_{t'}^2$ is the second derivative operator in fictitious time t' direction. After we make the connection between equations (3) and (7), (4) and (8), respectively, it is clear that the independent variable t' has the dimension of square root of the time *t*. Here E^U and H^U would behave as if they were propagating waves with a velocity of $(\mu\sigma)^{-1/2}$ in $m/\sqrt{s}$.

Mappings from the diffusive EM region to its corresponding fictitious wave domain can be accomplished by using a Laplace transform method [19], as follows

$$E=[1/(2t\sqrt{\pi t})]\cdot\int_0^\infty \exp[-(t')^2/(4t)]t'E^U\mathrm{d}t', \tag{9}$$

$$H=[1/(2t\sqrt{\pi t})]\cdot\int_0^\infty \exp[-(t')^2/(4t)]t'H^U\mathrm{d}t'. \tag{10}$$

When we substitute the constitutive relation $B=\mu_0 H$, we obtain

$$\begin{aligned}\partial_t B=\mu_0[(t')^2/(4t^2)-3/(2t)]/[2t\sqrt{\pi t}]\\ \cdot\int_0^\infty \exp[-(t')^2/(4t)]t'(\partial_t B)^U\mathrm{d}t'\end{aligned}, \tag{11}$$

where $\partial_t B$ and $(\partial_t B)^U$ are the electromotive force in real diffusive field and fictitious wave field, respectively.

Integral equations (9), (10) and (11) belong to the first class Fredholm integration equations, which are typical ill-posed equation produced by large amount of integral coefficient. Additionally, the TEM signals have a large dynamic time range, which also aggravate the weakness of this ill-posed problem. The inversion will be implemented by using PCGR method. The method can effectively decrease the condition number of coefficient matrix of integration equation and depress the ill-posed problem of the first class Fredholm integration equation.

Computing Fictitious Wave Fields

An important application of the correspondence principle of equations (9), (10) and (11) is constructing the data of fictitious wave field from TEM time signals.

Equations (9), (10) and (11) are written in numerical integration form

$$f(t)=\sum_{j=1}^n a(t,t'_j)u(t'_j)h_j, \tag{12}$$

where $f(t)$ is transient electric or magnetic field or induced electromotive force in real diffusive field. h_j is integral coefficient. $a(t,t'_j)$ is called the kernel function.

Writing equation (12) in matrix form

$$AU=F \tag{13}$$

where $A=[a\cdot h_j]$, the coefficient matrix A contains kernel function $a(t,t'_j)$ and integral coefficient h_j. U is fictitious wave field. F is TEM time signals.

In order to use the conjugate gradient (CG) method [21], equation (13) has to be converted to

$$A^{\mathrm{T}}AU = A^{\mathrm{T}}F\ . \tag{14}$$

As long as matrix A is a full column rank matrix, AA^{T} is a symmetric positive definite matrix. Fortunately, our matrix is a full column rank matrix, so equation (14) can be solved by CG method.

The operation from A to $A^{\mathrm{T}}A$ may considerably increase the condition number of matrix. To reduce the condition number of matrix and depress the ill-posed problem, the coefficient matrix AA^{T} is preconditioned before regularized conjugate gradient iteration. For the construction of preconditioners, which is easy to obtain, the symmetric successive over-relaxation (SSOR) precondition method is more effective, reducing the condition number of coefficient matrix effectively [22].

Assume that the preconditioner $M(v)$ is constructed through matrix $A(v)$, we construct the new equation (15)

$$M(v)^{-1}A(v)x = M(v)^{-1}(vx^{k} + f)\ , \tag{15}$$

where $A(v) = vI + A^{\mathrm{T}}A$, $f = A^{\mathrm{T}}F$, x^{k} is the value of fictitious wave field at the k-th iteration. Set initial value $x^{(0)}$ of x as unit vector. I is unit matrix. $M(v)$ is the preconditioner, whose expression is

$$M(v) = [(K + \omega C_{l})^{-1}K^{-1}(K + \omega C_{u})]/[\omega(2-\omega)]\ . \tag{16}$$

where K, C_l and C_u are the diagonal matrix, tril and upper triangular matrix, respectively, of the coefficient matrix $A(v)$. $\omega \in (0,2)$ is the relaxing factor. The matrix $M^{-1}A(v)$ approximates unit matrix, so the iteration converges fast. The specific process of SSOR preconditioning technique and RCG method can refer to [22] and [23].

The choice of the optimized regularization parameter v is very important. The regularization parameter v makes the fictitious wave field U optimize between approximation and stability. The regularization parameter not only affects the convergence and convergence speed, but also involves whether the solution is convergent to real solution of original problem. When v tends to infinity, it is equivalent to solve the minimum value problem of stabilization functional, and the new equation can be solved stably. However, it will lead to the solution that approach prior model completely, the observed data neglected and resolution reduced seriously. When v tends to zero, it means that it is based on the observed data completely. However, the variance of solution has been increased due to the discontinuity of inverse operator, resulting in instability or even failure. We would like to reference the paper of Wang [23] and some prior information for the choice of the optimized regularized parameter v. The regularization factor v is a quantity of a gradual change, and its initial value v_0 is the ratio of the data fitting functional to the stable functional. Based on a large number of previous simulation calculations, the initial value of the regularization parameter can be basically determined. The initial values of regularization parameters can be determined on the basis of a large number of simulation calculations in the early stage, and v_0=0.00005 can be obtained according to experience. In the subsequent iteration process, if the data fitting residuals gradually decrease with the number of iterations, the regularization factor can be kept unchanged, or else choose according to (16):

$$v = v_0\xi^{k}, k = 0,1,..., \tag{16}$$

where ξ is the empirical coefficient with $\xi > 1$, k represents the k-th iteration in the preconditioned regularization conjugate gradient (PRCG).

EXPERIMENTAL RESULTS AND ANALYSIS

In this section, some numerical experiments on synthetic wave field records and a theory model are given to analyze the characteristics of fictitious wave field and illustrate the performance of the proposed method.

Characteristics analysis of fictitious wave field

The fictitious wave field is recorded by Gaussian pulse as wavelet, and some layered models are simulated. Data transformation from the diffusive TEM region to the fictitious wave domain is implemented by PRCG method. A fixed frequency is taken as an example of the analysis in the interval [10us~10ms] of equidistant distribution, and the number of sampling points is M=101. In the range of [0.005~0.5], the fictitious time is discretized. To ensure that the coefficient matrix *A* is a full column rank matrix, the number of discrete points of the fictitious time is N=M=101. The blue solid line in Figure 1(a) is the synthetic wave field record of the D-type model. (D is a two-layer model name. The resistivity distribution of the D-type model is $\rho_1 > \rho_2$. ρ_1, ρ_2 is the resistivity of first layer, second layer, respectively.) The pulse peak fictitious time q1 corresponds with the first underground surface, and the sign of pulse amplitude corresponds with the resistivity relative change of layered model (The resistivity distribution of the G-type model is $\rho_1 < \rho_2$, G is a two-layer model name too, and its synthetic wave field record is shown in Figure 2.). The TEM signal decay curve of the D-type model is shown in Figure 1(b), where the blue dashed line shows the TEM signal decay curve of the uniform half-space model (*U*=1). It can be seen that as the layer resistivity decreases, the slope of the curve increases and the attenuation of TEM signal of the D-type model becomes slower. The red dashed line in Figure 1 (a) is the inversion result of fictitious wave field, which is consistent with the known fictitious wave field record. It shows that the proposed method is available in solving the fictitious wave field and improves the efficiency in fictitious wave field solve.

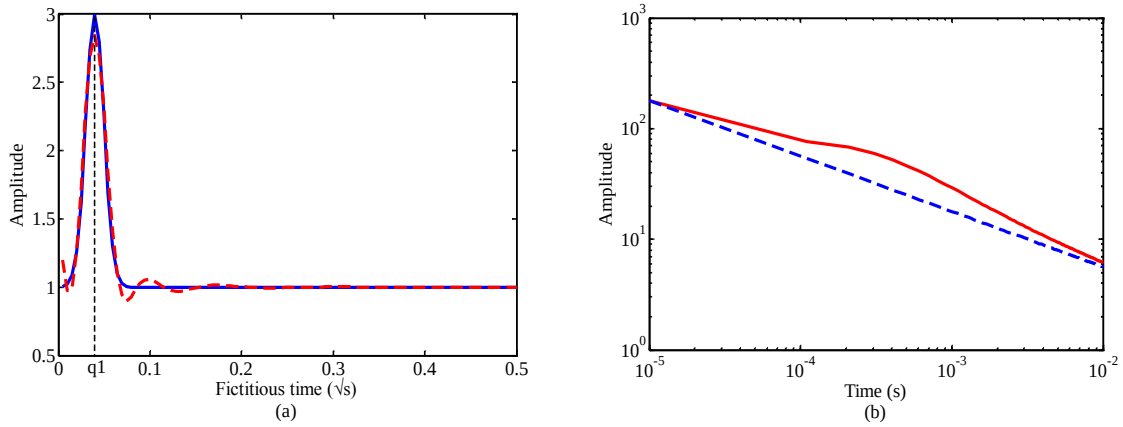

Figure 1: This is Results of the fictitious wave field transformation and inverse transformation of the D-type model (a) Synthetic fictitious wave field record of the D-type model and its results of the inverse transformation. The amplitude of pulse is A1=2, the width is w1=0.05, and the pulse peak fictitious time is q1=0.04. (b) Decay curve of TEM signal of the D-type model.

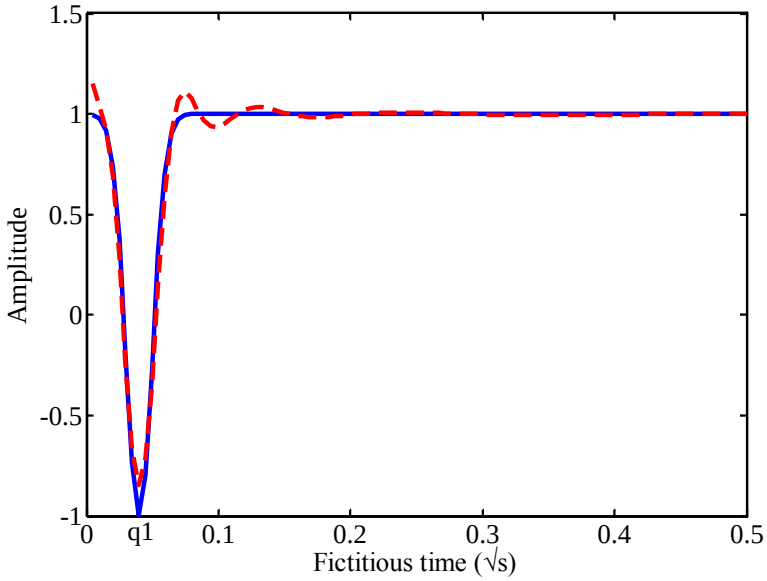

Figure 2: Synthetic fictitious wave field record of the G-type model and its results of inverse transformation. The amplitude of pulse is A1=-2, the width is w1=0.05, and pulse peak fictitious time is q1=0.04.

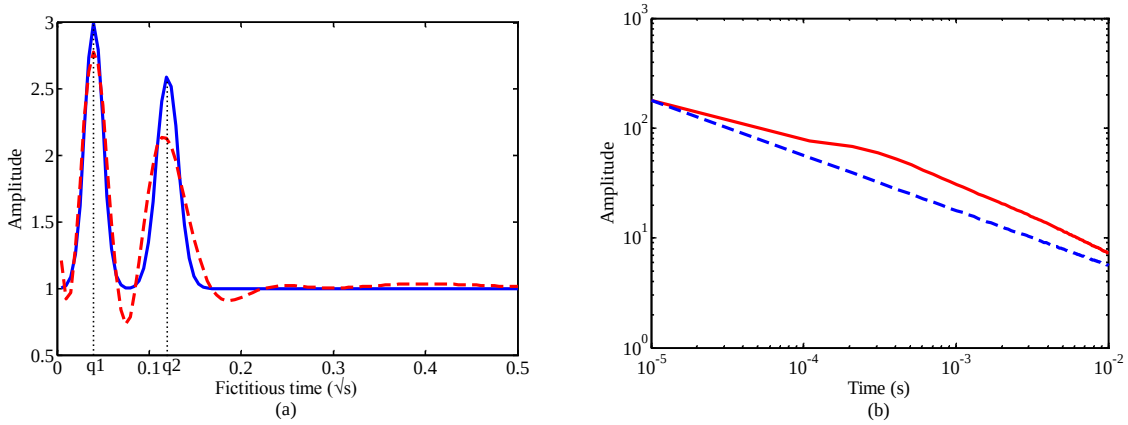

Figure 3: Results of the fictitious wave field transformation and inverse transformation of the Q-type model (a) Synthetic fictitious wave field record of the Q-type model and its results of inverse transformation. The first pulse amplitude is A1=2, the width is w1=0.05, and pulse peak fictitious time is q1=0.04. The amplitude of second pulse is A2=1.6, the width is w2=0.06, and pulse peak fictitious time is q2=0.12. (b) Decay curve of TEM signal of the Q-type model.

The blue solid line in Figure 3(a) is the synthetic wave field record of the Q-type model. (Q is a three-layer model name. The resistivity distribution of the Q-type model is $\rho_1 > \rho_2 > \rho_3$. ρ_1, ρ_2, ρ_3 is the resistivity of first layer, second layer, third layer, respectively.) The pulse peak fictitious time q1 corresponds with the first underground surface. And q2 is the fictitious time corresponding with the second underground surface. The decay curve of TEM signal of the Q-type model is shown in Figure 3(b), where the blue dashed line is the TEM signal decay curve of the uniform half-space model (U=1). As the layer resistivity decreases, the attenuation of TEM signal of the Q-type model slows

down. The red dashed line in Figure 3(a) is the result of inversion. The first pulse is in good agreement with the known wave field record. The second pulse amplitude has a great attenuation compared with the first pulse amplitude, and the wavelet width is slightly increased, which is consistent with the propagation law of the wave in heterogeneous medium, thus proving the correctness of the algorithm. On the other hand, the inversion result shows that TEM method has higher resolution of shallow anomaly. With the increase of depth, the high frequency component of TEM signal is seriously lost, and the response is mainly in low frequency range, so the resolution of deep anomaly is reduced.

Analysis of Wave Field Transformation Results of theory Model

We put a low resistivity target into a half space, and take it as a theory model to test the preconditioned regularized conjugate gradient fictitious wave domain (PRCG-FWD) method. The resistivity of the half space is 50 Ω·m. The resistivity of the target is 5 Ω·m, the size is 80 m × 80 m × 50 m, and its buried depth is 100 m. The position of the transmitter loop and survey line is shown in Figure 4. There are five survey lines, and each with 11 survey points. The line space and point distance are both 20 m.

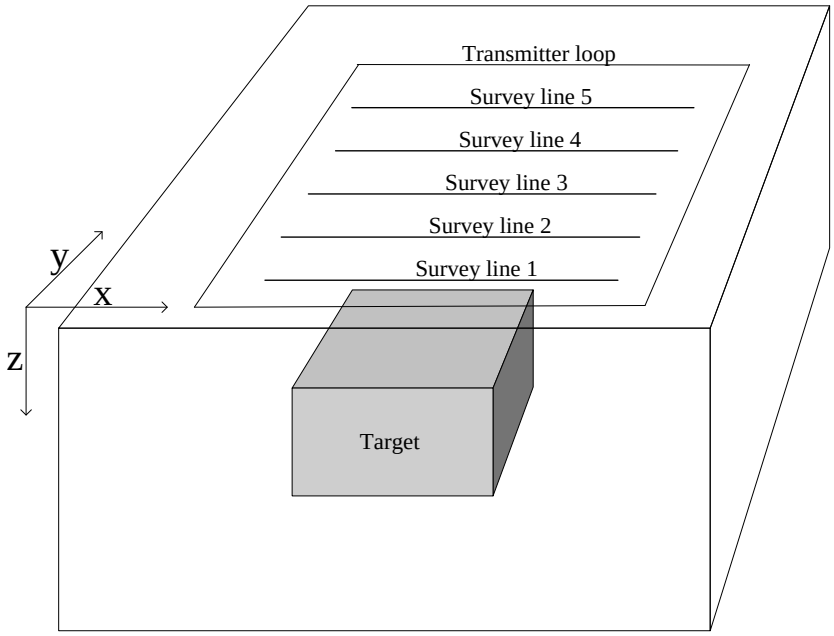

Figure 4: Low resistivity target into a half space and the surface line. The gray block in the figure is the underground target, the size is 80 m × 80 m× 50 m and the buried depth is 100 m. The line space and point distance are both 20m.

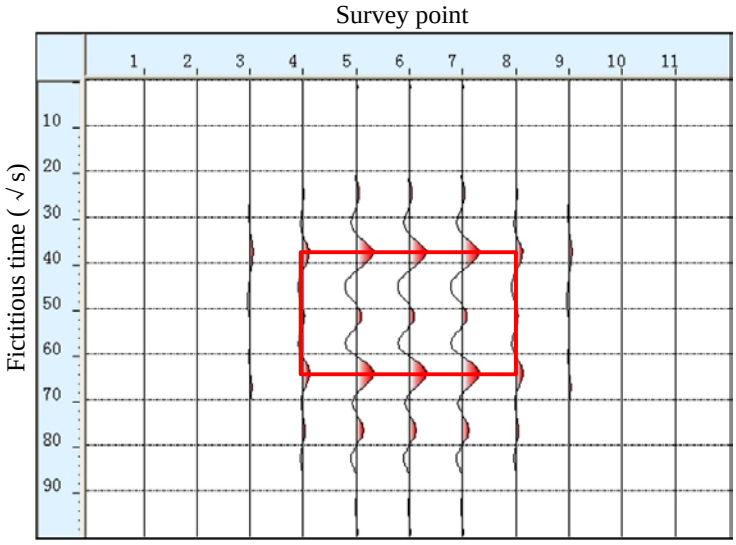

Figure 5: Results of fictitious wave field of the survey line 3.

With the FDTD forward modelling algorithm, we acquire the response of those survey points, and transform them to the fictitious wave field. The fictitious wave field of the typical survey line is shown in figure 5, and we can see the boundary of the underground target. In figure 5, the vertical axis is the fictitious time. In order to get the actual depth of underground objects, we need to do velocity analysis and Kirchhoff migration imaging. The velocity of fictitious wave field is a quantity related to the resistivity of underground medium. After migration imaging, the depth profile should be similar to the theory model. In summary, this method is correct and effective. It can be well used for fictitious wave field transformation of TEM signal.

CONCLUSIONS

In this paper, we propose a PRCG-FWD method for TEM response of conductive media modeling and inversion. The integral equations of the correspondence principle relating the diffusive fields and fictitious wave fields are derived. Considering the integral equation belongs to the first class Fredholm integration equation which is a typical ill-pose problem, we use the over-relaxation PCGR method, which can effectively reduce the condition number of coefficient matrix of integration equation and depress the ill-posed problem. The scheme avoids segmentation of TEM time signals by the method of conventional regularization [20] due to a large dynamic time range. Applications on synthetic wave field records and the theory model show that the proposed method can achieve a good performance. The obtained fictitious wave fields not only satisfy the wave equation, but also have the propagation characteristic of the wave similar to the seismic wavelet. It provides a good basis for the subsequent use of the wave equation migration imaging method.

ACKNOWLEDGEMENTS

The research is supported by the National Natural Science Foundation of China under Grant 61761009, 61102115, 61362020. (Corresponding author: Guofu Wang.)

REFERENCES

[1] M. Nabighian, “Comment on "Electromagnetic geophysics: Notes from the past and the road ahead,” Geophysics, vol. 77, no. 4, pp. X3-X6, 2012.

[2] D. Yang and D. W. Oldenburg, "Three-dimensional inversion of airborne time-domain electromagnetic data with applications to a porphyry deposit," Geophysics, vol. 77, no. 2, pp. B23-B34, 2012.

[3] R. Streich, "Controlled-Source Electromagnetic Approaches for Hydrocarbon Exploration and Monitoring on Land," Surveys in Geophysics, vol. 37, no. 1, pp. 47-80, 2016.

[4] A. V. Christiansen, E. Auken, and K. Sørensen, "The transient electromagnetic method," Groundwater Geophysics: A Tool for Hydrogeology, Berlin, Heidelberg: Springer. pp. 179-226, 2009.

[5] M. Chongo, A. Vest Christiansen, A. Tembo, K. E. Banda, I. A. Nyambe, and F. Larsen, et al., "Airborne and ground-based transient electromagnetic mapping of groundwater salinity in the Machile–Zambezi Basin, southwestern Zambia," Near Surface Geophysics. vol. 13, no. 4. pp. 383-396, 2015.

[6] M. Hatch, T. Munday, and G. Heinson, "A comparative study of in-river geophysical techniques to define variations in riverbed salt load and aid managing river salinization," Geophysics, vol. 75, no. 4, pp. WA135-WA147, 2010.

[7] P. S. a. D. Irawan, "Static Electrode DC Resistivity Measurement at Surface Water for Pond Subsurface Layer Imaging," IOP Conference Series: Earth and Environmental Science, vol. 29, no. 1, p. 012024, 2016.

[8] H. Sun, X. Li, S. Li, Z. Qi, M. Su, and Y. Xue, "Multi-component and multi-array TEM detection in karst tunnels," Journal of Geophysics and Engineering, vol. 9, no. 4, pp. 359-373, Aug 2012.

[9] Z. P. Qi, X. Li, X. S. Lu, Y. Y. Zhang, and W. H. Yao, "Inverse transformation algorithm of transient electromagnetic field and its high-resolution continuous imaging interpretation method," Journal of Geophysics and Engineering, vol. 12, no. 2, pp. 242-252, 2015.

[10] X. Li, G. Xue, and C. Yin, "Development and Prospect of Transient Electromagnetic Method," Singapore: Springer Singapore, pp. 1-16, 2017.

[11] A. P. Raiche, "An integral equation approach to 3D modeling," Geophys. J. Roy. Astr. Soc., vol. 36, no. 1, pp. 363-376, 1974.

[12] Y. Sasaki, M. J. Yi, J. Choi, and J. S. Son, "Frequency and time domain three-dimensional inversion of electromagnetic data for a grounded-wire source," Journal of Applied Geophysics, vol. 112, pp. 106-114, 2015.

[13] I. K. Reddy, R. J. Phillips, and D. Rankin, "Three-dimensional modelling in magnetotelluric and magnetic variational sounding," Geophys. J. Roy. Astr. Soc., vol. 51, no. 2, pp. 313-325, 1977.

[14] M. M. Goldman and C. H. Stoyer, "Finite‐difference calculations of the transient field of an axially symmetric earth for vertical magnetic dipole excitation," Geophysics, vol. 48, no. 7, pp. 953-963, 1983.

[15] L. H. Cox, G. A. Wilson, M. S. Zhdanov, "3D inversion of airborne electromagnetic data," Geophysics, vol. 77, pp. WB59-WB69, 2012.

[16] Y. Ji, Y. Hu, and N. Imamura, "Three-Dimensional Transient Electromagnetic Modeling Based on Fictitious Wave Domain Methods," Pure and Applied Geophysics, vol. 174, no. 5, pp. 2077-2088, 2017.

[17] G. Kunetz, "Processing and interpretation of magnetotelluric soundings," Geophysics, vol. 37, no. 6, pp. 1005-1021, 1972.

[18] M. M. Lavrent′ev, V. G. Romanov, and S. P. Shishat•skiĭ, "Ill-posed problems of mathematical physics and analysis," (in Russian), Providence RI: American Mathematical Society, 1986.

[19] K. H. Lee, G. Liu, and H. F. Morrison, "A new approach to modeling the electromagnetic response of conductive media," Geophysics, vol. 54, no. 9, pp. 1180-1192, 1989.

[20] X. Li, G. Q. Xue, J. P. Song, W. B. Guo, and J. J. Wu, "An optimize method for transient electromagnetic field-wave field conversion," (in Chinese with English abstract), Chinese J. Geophys., vol. 48, no. 5, pp. 1185-1190, 2005.

[21] Z. Bai. S. Zhang, "A regularized conjugative gradient method for symmetric positive definite system of linear equations," J. Computational Mathematics, vol. 20, no. 4, pp. 437-448, 2002.

[22] Ru-Shan Chen, Edward Kai-Ning Yung, Chi H. Chan, Dao Xiang Wang, and Da Gang Fang, Application of the SSOR preconditioned CG algorithm to the vector FEM for 3D full-wave analysis of electromagnetic-field boundary-value problems. IEEE Transactions on Microwave Theory and Techniques, vol. 50, no. 4, pp. 1165-1172, 2002.

[23] Y. F. Wang, "A restarted conjugate gradient method for ill-posed problems," Acta Mathematicae Applicatae sinica (English Series), vol. 19, no. 1, pp. 31-40, 2003.

Editor's note.
This paper may be referred to, in other articles, as:

Xiaoyu Zhao, Guofu Wang, Faquan Zhang, Jincai Ye, and Yiyu Zhan: "Transient Electromagnetic Response of Conductive Media Modeling and Inversion Based on Fictitious Wave Domain Method" *Electronic Journal of Geotechnical Engineering*, 2018 (23.01), pp 21-30. Available at ejge.com.